Investigation of the Mixing- and Devolatilization Behavior in a Continuous Twin-Shaft Kneader

Oliver Seck,[1] *Tobias Maxisch,*[1] *Hans-Joachim Warnecke,**[1] *Dieter Bothe**[2]

Summary: The technical synthesis and processing of polymer materials is the basis for major branches of the chemical industry. Well introduced for high-viscosity processes are screw extruders. However, in case of large residence times a large volume kneader is more appropriate, but the latter still requires further understanding for intensification purposes. To achieve this, silicone oil of high viscosity is used as kneading material. First, the axial mixing behavior is characterized by studying the residence time distribution. The response functions show that the classical dispersion model leads to an appropriate description of the experimental data. By means of a fast chemical reaction of second order the radial mixing behavior including transport on the molecular scale is studied. The amount of detected product is a measure for the contact-area produced by kneading and therefore for the mixing efficiency. Furthermore, the mass transfer from the silicone oil phase to the gas phase is investigated in two cases. Firstly, the transfer component is dissolved in the liquid phase and, secondly, it is dispersed in it. Both industry relevant cases are experimentally and theoretically investigated. The kneader enables high surface renewal and larger concentration gradients for the efficient mass transfer.

Keywords: devolatilization; kneader; mass transfer; mixing; polymerization

Introduction

For the production of various commodities and polymers machines are required which can handle high viscous materials in continuous operation,[1,2] not only for radial mixing to achieve homogeneous reaction conditions, but also for devolatilization during or after the reaction. For such purposes a thorough self-cleaning of the reaction chamber is necessary to ensure that no adhesion or dead zones occur in the machine.[3] In case of large residence time twin-shaft kneaders are more appropriate than extruders due to their larger free volume.[4] The decoupling of rotational frequency and throughput offers advantages, too. These features allow for diverse operation modes for production and processing.

Due to their advantages and the good performance in mixing, kneaders of all types are common tools not only in industrial processes but also in scientific work. The usage of kneaders is mentioned by various authors in many work fields. For example in modification of polymers,[5–7] molding[8–9] or even pharmaceutics.[10] Besides this, kneaders are also used for production of polymers.[11] Thus, kneaders are commonly used but they are neither well understood nor deeply investigated.

In contrast, in case of twin-screw extruder as a similar device both experimental and theoretical works are well known. One of the main topics in experimental work is the investigation of the axial mixing behavior

[1] Institute of Polymer Materials and Processes, University of Paderborn, Warburgerstr. 100, 33098 Paderborn, Germany
E-mail: warnecke@tc.upd.de
Fax: (+49) 5251 603244;
[2] Mathematical Modeling and Analysis, Cluster of Smart Interfaces, Technical University Darmstadt, Petersenstr. 32, 64287 Darmstadt, Germany
E-mail: bothe@csi.tu-darmstadt.de

in terms of residence time distribution. Many approaches for various applications are reported in [12–17]. In a few articles these methods are extended to some specific types of kneaders,[18,19] but investigations concerning twin-shaft kneaders are not reported.

Radial mixing has been investigated with several techniques in stirred tanks[20,21] and in static mixers.[22] In case of extruders these techniques are reported, too[23,24], but not in case of twin-shaft kneaders.

The same can be stated concerning theoretical work. Early investigations in modeling extruders and some types of kneaders are based on simplified approaches like tanks in series[25] or superposition of basic transport functions.[26,27] Later work employs more sophisticated approaches, for example the combination of flow fields for single elements obtained by CFD-calculations with a cluster model[28] or direct numerical simulation combined with mapping techniques.[29,30]

But, due to their complex structural shape no results have been reported up to now concerning twin-shaft kneaders.

Regarding devolatilization of the kneading material, the mechanisms of mass transfer of dissolved components to be removed has to be considered. Investigations of the devolatilization process in twin-screw reactors are reported mainly since the 1990s. Besides experimental works[31–33] on mass transfer both with and without bubbles these papers also provide modeling approaches.[34–37] Still, an investigation for twin-shaft kneaders is missing. First steps in this direction are carried out in the present work for two different cases: Either the component is completely dissolved in the kneading material or it is dispersed as a second phase.

Due to the deep knowledge developed over decades, industry still prefers screw machines to kneaders and designs the latter mainly based on empirical knowledge. A profound understanding of the involved mixing processes is still lacking. Therefore, the aim of this work is to develop experimental methods which allow for the model based examination of the mixing and devolatilization behavior in a continuously operated twin-shaft kneader.

Experimental set-up

The twin-shaft kneader as a continuous chemical reactor for highly viscous fluids used here consists of two co-rotating shafts equipped with self-cleaning kneading elements (Figure 1).

Each kneading element carries a disc with five bars attached to it's edge. The encounter of two corresponding bars from the two shafts causes primarily the kneading effect and is defined as *one* kneading step. Hence, the geometrical design results in five kneading steps per rotation.

The schematic set-up of the continuous twin-shaft kneader is shown in Figure 2.

The kneading tools are located in the reaction chamber R which has a volume of $V_{reac} = 5$ L. Silicone oil with a viscosity of $\eta = 100$ Pa s is used as kneading material. It is pumped out of the 250 L storage tank T1 into the reaction chamber by a system of two gear pumps (P1, P2). The mass flow of the silicone oil is adjusted by the performance of the pumps and is independent on the frequency of the rotating shafts driven by the motor M. The weir W at the outlet of the apparatus serves for setting the filling level. The injector I allows for tracer impulse input at the inlet of the reaction chamber. The Pumps P3 and P4 enable to add continuously two independent side flows of tracer from tank T2, resp. T3.

Axial Mixing

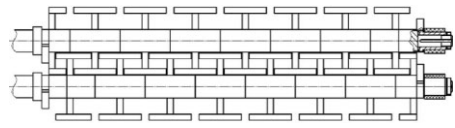

Figure 1.
Top view on shafts equipped with kneading elements.

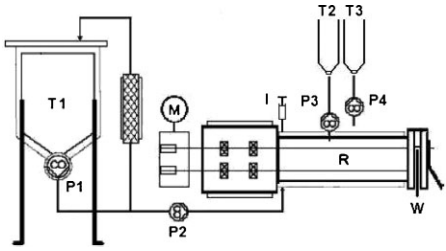

Figure 2.
Schematic experimental set-up.

To determine the axial mixing behavior the kneader is operated continuously. The tracer Sudan® Yellow 3G is dosed by pressure impulse via injector I. At the outlet of the kneader samples are taken and their mass load X of tracer in dependence on time is measured via photometry at a wavelength of $\lambda = 405$ nm. The mass flow $\dot{m}$ of silicone oil and the rotational frequency n of the mixing tools are varied and account together with the height of the weir for the adjustment of a defined filling level.

First, to normalize the measured response function curves the mean residence times $\bar{t}$ are calculated. They result from the discrete first moment of the distribution of the tracer load X_i in each individual sample at constant time intervals and the individual residence time t_i according to eq. (1)

$$\bar{t} = \frac{\sum_i t_i X_i}{\sum_i X_i}. \quad (1)$$

The degree of axial backmixing can be described by the Bodenstein number Bo. Low Bodenstein numbers less than 1 indicate high backmixing and values higher than 100 correspond to plug flow behavior, i.e. to marginal backmixing. According to the axial dispersion model for a bilaterally closed reactor, the Bodenstein number is determined by the normalized variance of the impulse function[38]:

$$\sigma_\theta^2 = \frac{2}{Bo} - \frac{2}{Bo^2}[1 - \exp(-Bo)] \quad (2)$$

Table 1.
Axial mixing parameters in dependence on mass flow and rotational frequency

$\dot{m}_{PDMS}$ [kg h^{-1}]	n [min^{-1}]	γ [–]	$\bar{t}$ [min]	Bo [–]
1.89	40	0.51	80.4	31.0
3.12	5	0.77	71.4	77.0
3.12	22	0.63	56.8	43.0
3.12	40	0.53	51.4	36.0
5.26	5	0.90	48.9	53.0
5.23	22	0.68	37.7	58.5
5.25	40	0.60	34.2	42.0
7.07	22	0.66	27.7	53.0
7.06	40	0.64	27.1	45.5
10.51	40	0.67	17.6	47.5

with

$$\sigma_\theta^2 = \frac{\sum_i t_i^2 X_i}{\bar{t}^2 \sum_i X_i} - 1 \quad (3)$$

and

$$\theta = \frac{t}{\bar{t}}. \quad (4)$$

For a totally opened weir the resulting filling levels γ, mean residence times, and Bodenstein numbers are summarized in Table 1.

Passing through the reaction chamber the silicone oil is affected by successive kneading steps. The overall number of effective kneading steps $\overline{U}$ results from five kneading steps per rotation multiplied by the mean residence time, hence

$$\overline{U} = 5\, n\, \bar{t}. \quad (5)$$

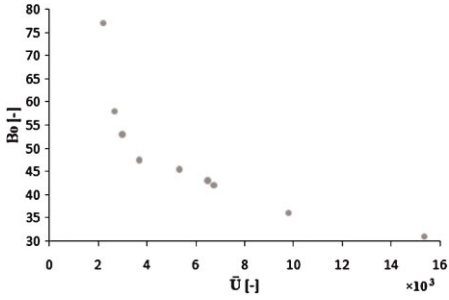

Figure 3.
Bodenstein number as a function of the effective number of kneading steps.

The dependence of the Bodenstein number on the number of effective kneading steps $\overline{U}$ is shown in Figure 3.

The decrease of the Bodenstein number qualitatively indicates an increase in backmixing due to kneading.

Radial Mixing

To achieve a narrow molecular weight distribution of the polymer, a fast homogenization of the reactants in cross sectional direction is required. Therefore fast radial mixing is highly important.

At first, radial mixing is studied at zero mass flow, i.e. in batch mode. Here the experimental investigation of the radial mixing behavior is realized by stacking homogeneous layers of silicone oil charged, resp. uncharged with tracer. The stacked volumes are mixed by kneading and the quality of the mixture is analyzed. Samples at three different radial positions are taken in dependence on the number of kneading steps U. Because back mixing is small, it is possible to take sample triples at different axial positions during a single experiment instead of taking samples time-dependent at the same position.

Initially a non-reactive tracer is used to characterize mixing solely on macro scale. In this case a layer of silicone oil charged with Sudan® Red 7B is followed by an uncharged one. The taken samples are measured by means of photometry at a wave length of $\lambda = 525$ nm.

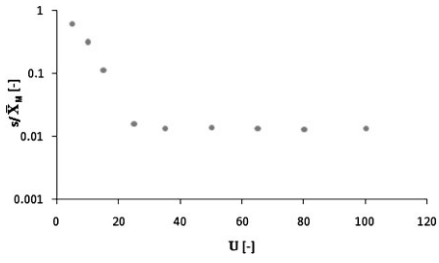

Figure 4.
Radial macro mixing: variation coefficient of tracer load as a function of kneading steps.

Figure 4 shows that homogenization on the macro scale sets in after approximately 25 kneading steps shown by the variation coefficient criterion $s\overline{X}_M^{-1} < 0.01$. Each value of the variation coefficient is calculated by the mass load variance s of each radial sample triple divided by the theoretical average mass load $\overline{X}_M$.

By means of a fast chemical reaction of second order type

$$A_1 + A_2 \rightarrow P \tag{6}$$

the radial mixing behavior is studied including transport down to the molecular scale. Since the two reactants cannot coexist they react directly at the contact-area between two fluid elements, each one charged with one of the reactants. Thus, the amount of generated product is a measure of the contact-area produced by kneading and characterizes the advance in mixing.

An appropriate chemical reaction for (6) is the deprotonation-reaction (Figure 5) of 2-nitrophenol (2NPH) with dibutylamine (DBA), because all reactants are soluble in silicone oil and the product $2NP^-$ can be detected by means of VIS-photometry at $\lambda = 445$ nm simultaneously with the educts which are measured at $\lambda = 405$ nm.

The experiments are carried out by stacking two layers, one for each educt. To prevent early reaction by diffusion before start, they are separated by an additional thin protection layer. The sampling procedure is the same as described above.

The development of the variation coefficient of mass load of the product (Figure 6) describes the mixing down to micro scale. Whereas the corresponding quantity of the educt shows the progress of

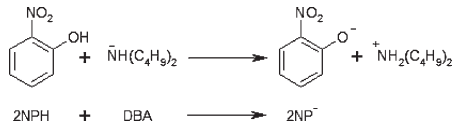

Figure 5.
Acid-base- reaction of 2-nitrophenol and dibutylamine.

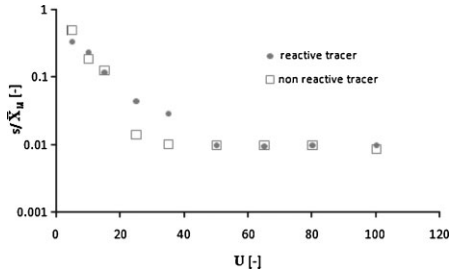

Figure 6.
Macro and micro mixing: variation coefficient of non reactive and reactive tracer load as a function of kneading steps.

mixing on macro scale as investigated with Sudan® Red 7B before.

The generation of product and, hence, the homogenization is finished after about 50 kneading steps according to the same variation coefficient criterion of $s\,\overline{X}_M^{-1} < 0.01$.

In continuous mode, mass flow is passing axially the apparatus, so that mixing and reaction are studied in dependence on reactor length z. Both kinds of experiments with reactive and non-reactive tracer are realized by a main flow of silicone oil on which one, resp. two side flows, loaded with tracer, are added. The flow rates are totally independent on each other and their dosage occurs at the same axial position $z = 0$.

The radial distribution of the tracers occurs fast due to rotation of the kneading elements. In axial direction the distribution occurs by mass flow. After reaching steady state, samples are taken along axial position. The tracer load is analyzed by photometry. The stationary normalized load profiles $X\,\overline{X}_M^{-1}$ of the educt and of the generated product are exemplarily shown in Figure 7.

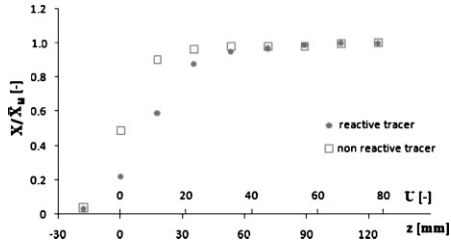

Figure 7.
Axial macro and micro mixing: normalized non reactive and reactive tracer load as a function of axial position, resp. number of kneading steps.

The load profile of the non-reactive tracer shows a stronger rise than the one of the generated product, because the latter also takes into account transport down to the molecular scale. For the chosen conditions, the reactive tracer has reacted to completion after a distance of $z = 84\,\text{mm}$ which equals $U = 53$. The non-reactive curve reaches its asymptotic value after a distance of $z = 40\,\text{mm}$ corresponding to $U = 25$.

As tracer is found even at a position $z < 0$ small effects of backmixing are observed.

Devolatilization

Devolatilization of high viscous material is an important downstream process as well as an essential step for polymerization. To understand and describe the basic mechanism of devolatilization in a twin-shaft kneader, the mass transfer behavior is investigated experimentally. Concerning the component which has to be removed it is important to discriminate if the component is dissolved or dispersed in the kneading material.

An example for devolatilization of a dissolved component is the removal of monomer or solvent after polymerization to improve the product quality.

In case of polycondensation, insoluble molecules are generated and dispersed, e.g. water. For economic reasons the condensate has to be removed to shift the equilibrium of reaction to the product side. The process efficiency increases with the volatility of the contamination because of higher vapor pressure.

Concerning the main parameters of this study - rotational frequency and mass flow - twin-shaft kneaders offer two advantages in comparison to screw-extruders:

1. The mass flow is independent of the rotational frequency.
2. Kneaders are operated with a filling level $\gamma < 70\%$, so the remaining part of

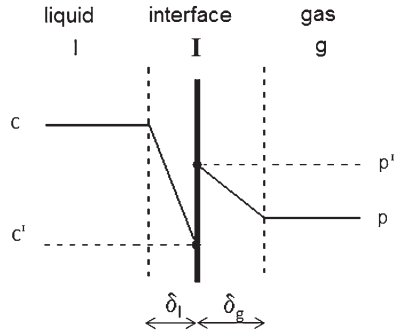

Figure 8.
Concentration profiles according to film theory.

the reaction chamber serves for devolatilization. In contrast to extruders, no separate devolatilization chamber is required. The devolatilization length l_{gas} is equal to the length of the mixing chamber l_{reac}.

By rotation of the shafts the mass transfer between the kneading material and the gas phase is enhanced due to the generation of stretched and thinned fluid films.

For the evaluation of the experiments, the two-film theory[39,40] is used as basic model (Figure 8).

Assuming stagnant fluid films on both sides of the interface I, the molar flux J [mol $s^{-1}m^{-2}$] of the transfer component occurs due to molecular diffusion according to Fick's first law

$$J = D_l \frac{c - c^I}{\delta_l} = \frac{D_g}{RT} \frac{p^I - p}{\delta_g} \tag{7}$$

with D diffusion-coefficient, c concentration, p partial pressure, δ layer thickness, R universal gas constant, T temperature, i index: g gas phase, l liquid phase. The quotient

$$k_i = \frac{D_i}{\delta_i} \tag{8}$$

yields the mass transfer coefficient k. Taking into account phase equilibrium at the interface described by Henry's law

$$p^I = H\, c^I, \tag{9}$$

with H the respective Henry's law constant, this enables to eliminate the interface concentration, resp. pressure and leads to

$$J = \frac{1}{\frac{1}{k_l} + \frac{RT}{H}\frac{1}{k_g}} \left(c - \frac{p}{H}\right). \tag{10}$$

Then, the mass flow $\dot{m}$ of the transfer component yields from

$$\dot{m} = J\, A\, M \tag{11}$$

with A interfacial area and M molecular weight. Introducing the specific interfacial area a

$$a = \frac{A}{\gamma\, V_{reac}} \tag{12}$$

leads to

$$\dot{m} = J\, a\, \gamma\, V_{reac}\, M \tag{13}$$

and

$$\dot{m} = \frac{M\, \gamma\, V_{reac}}{\frac{1}{k_l a} + \frac{RT}{H}\frac{1}{k_g a}} \left(c - \frac{p}{H}\right). \tag{14}$$

Equation (14) is the basic equation to determine the specific mass transfer coefficient k_l a, resp. k_g a.

Devolatilization of a Dissolved Component

Due to the significant difference of the viscosity of both involved phases it is assumed that the main barrier for diffusive mass transport lies on the liquid side, so molar transfer resistance on the gaseous side is negligible, i.e.

$$\frac{1}{k_l a} \gg \frac{RT}{H}\frac{1}{k_g a}. \tag{15}$$

Thus, equation (14) reduces to

$$\dot{m} = M\, \gamma\, V_{reac}\, k_l\, a \left(c - \frac{p}{H}\right). \tag{16}$$

To simplify the evaluation, the concentration is kept constant by choosing a material system with low partial pressure of the transferred component. Furthermore, p is adjusted to zero by continuously eliminating the transferred component from the gas phase by reactive absorption

which additionally enhances the analytic sensitivity significantly.

Here, the chemical reaction of 2-nitrophenole 2NPH and dibutylamine DBA (Figure 5) is used again. It offers the following advantages: The vapor pressure of 2NPH is very low ($p_{2NPH,g} = 6.9\,Pa$, $T = 20\,^{\circ}C$),[41] so that its concentration in the high viscous bulk phase does not change detectably. The reactive absorption of gaseous 2NPH in the DBA leads to $p = 0$. Thus, with the mass concentration β!

$$\beta = M\,c\,[kg\,m^{-3}] \tag{17}$$

equation (16) simplifies to

$$\dot{m} = \gamma\,V_{reac}\,k_l\,a\,\beta. \tag{18}$$

The transferred mass m_{2NPH} is determined by VIS photometry at a wavelength of $\lambda = 405\,nm$.

Firstly, batch mode experiments are done by filling the kneader with a mass $m = 3.0\,kg$ of 2NPH silicone oil solution with a mass concentration $\beta_{2NPH,0} = 0.2\,g\,L$. Above the liquid phase a cuevette filled with dibutylamine ($V_{DBA} = 3.0\,mL$) is placed. Then the liquid phase is mixed and finally, the machine is sealed and devolatilization starts. The operating conditions are $T = 20\,^{\circ}C$ and $p^{*} = 1013\,mbar$.

The experimental set-up is shown in Figure 9.

The values of mass concentration β of product $2NP^{-}$ in DBA in dependence on time and rotational frequency of the kneading tools are shown in Figure 10.

The curves for different frequencies show a sigmoidal progression, with a small

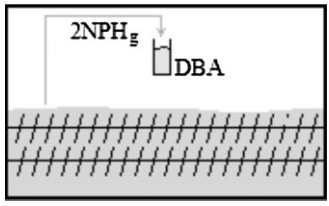

Figure 9.
Schematic set-up for devolatilization of a dissolved component.

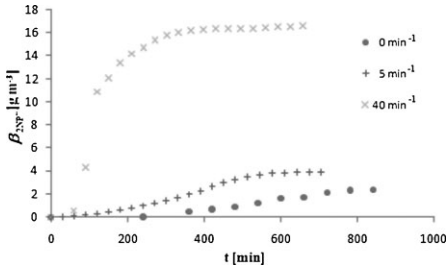

Figure 10.
Mass concentration of 2-nitrophenol degassed from silicone oil in dependence on time at different rotational frequencies.

almost linear regime near the inflection point.

The 2NPH mass flow can be calculated from the slope of the curves in the linear regime and enables the evaluation of the transfer coefficient k_l a. The results are shown in Table 2.

As shown in Table 2 a higher rotational speed results in a larger k_l a value.

Note that in case of no rotation ($n = 0\,min^{-1}$) a free surface exists. Then the order of magnitude of k_l a can be estimated by

$$k_l\,a = \frac{D\,A}{\delta\,V_{reac}\,\gamma}. \tag{19}$$

Using the estimated values $D = 10^{-14}\,m^2$, $A = 814\,cm^2$ and $\delta = 1\,mm$ yields

$$k_l\,a = 10.8 \times 10^{-10}\,s^{-1}. \tag{20}$$

This estimated value supports reliably of the experimental values.

For devolatilization of a dissolved component the deprotonation of 2-nitrophenol is an efficient method. However, the resulting mass transfer coefficients are very small compared to mass transfer usually found in industrial devolatilization pro-

Table 2.
Mass transfer parameters for the devolatilization of dissolved 2-nitrophenol in silicone oil

$n[min^{-1}]$	$\dot{m}_{2NPH}[g\,s^{-1}]$	$k_l\,a\,[s^{-1}]$	$(k_l\,a)^{*}\,[-]$
0	1.86×10^{-10}	3.1×10^{-10}	1.00
5	3.68×10^{-10}	6.1×10^{-10}	1.97
40	47.78×10^{-10}	79.6×10^{-10}	25.67

cesses, due to extremely low diffusion coefficients. Therefore, a transfer component of higher volatility and faster diffusion in silicone oil has to be chosen. N-heptane dissolved in silicone oil is appropriate. The analysis is performed by combining weighing of the condensed n-heptane transferred into cooling traps and headspace gas chromatography of its content in the liquid phase.

First exploratory experiments show a fast mass transfer of n-heptane and hence a more efficient discharging in comparison to 2-Nitrophenol.

Devolatilization of a Dispersed Component

For gathering general knowledge of devolatilization of a dispersed component, the kneader is operated on batch mode. For this purpose the experimental set-up is supplemented by a vacuum pump and three cooling traps in series (Figure 11).

In order to achieve a dispersion with a starting load of $X_{H20,0} = 0.1$, silicone oil ($m = 3{,}0\,kg$) is filled into the kneader followed by water (mass $m_{H20,0} = 300\,g$). Finally, the kneader is sealed and devolatilization starts. The operating conditions are: temperature $T = 80\,^{\circ}C$, system pressure $p^{*} = 100$ mbar.

In dependence on time and rotational frequency, the degassed amount of water is condensed in the cooling traps and determined by weighing. A relative mass of 95% is found in the first trap, the remaining mass is found in the second one. The third trap is uncharged, which indicates that all mass has been trapped.

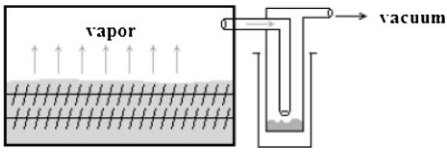

Figure 11.
Schematic set-up for devolatilization of a dispersed component.

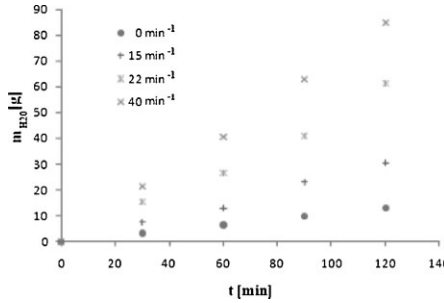

Figure 12.
Mass of degassed water in dependence on time at different rotational frequencies.

The experimental results qualitatively show an increase of devolatilization efficiency at higher temperature and lower system pressure. The transferred mass in dependence on devolatilization time and on rotational frequency is shown in Fig 12.

It shows a linear dependence of mass on devolatilization time as long as the amount of dispersed water in silicone oil does not change significantly. Concerning rotational frequency, a higher speed results in a higher mass transport. To achieve reliable results experiments are stopped after a relative mass transfer of 25% in order to keep the system pressure constant.

Due to the fact that water is not soluble in silicone oil mass transport within the liquid phase does not exist. Water on the surface moves directly into the gas phase as the vapor pressure of water is $p_{H_2O,g} = 473\,mbar$ at $T = 80\,^{\circ}C$ and the system pressure is $p^{*} = 100\,mbar$.

Thus, k_l a vanishes in equation (14) and results in

$$\dot{m} = \frac{k_g\, a\, M\, \gamma\, V_{reac}}{R\, T}\,(c\, H - p). \tag{21}$$

The product c H has to be replaced by the partial pressure of H_2O and p by the system pressure. This leads to the evaluation equation for k_g a

$$\dot{m}_{H20} = \frac{M_{H20}\, k_g\, a\, V_{reac}\, \gamma}{R\, T}\left(p_{H_2O,g} - p^{*}\right). \tag{22}$$

The mass flows $\dot{m}_{H2O}$ follow from the slopes in Figure 12.

Table 3.
Mass transfer parameters for degassing dispersed water from silicone oil

$n\,[\mathrm{min}^{-1}]$	$\dot{m}_{H2O}[\mathrm{g\,s}^{-1}]$	$k_g\,a[\mathrm{s}^{-1}]$	$(k_g\,a)^*$ [–]
0	1.77×10^{-6}	2.57×10^{-3}	1.00
15	4.13×10^{-6}	6.01×10^{-3}	2.34
22	8.32×10^{-6}	12.12×10^{-3}	4.72
40	11.66×10^{-6}	16.99×10^{-3}	6.61

Table 3 summarizes the data of mass flow, mass transfer coefficients k_g a and transfer coefficients related to k_g a at $n = 0\,\mathrm{min}^{-1}$ $(k_g\,a)^*$.

As expected, higher rotational speed results in larger transfer coefficients k_g a. The kneader works more efficiently at moderate frequencies.

The presented method to evaluate the devolatilization behavior is suitable to investigate the influence of the structural shape of the kneading elements on the apparatus performance.

Conclusion

New techniques are developed to investigate the mixing- and devolatilization behavior in high viscous liquids in twin-shaft kneaders. They allow for determining mixing in axial and radial direction on macro scale as well as down to micro scale. In the latter case a reactive tracer is used.

The results show that radial mixing is fast and therefore no cross-sectional concentration gradients exist. Thus, the kneader almost behaves like a plug flow reactor. The mixing process down to micro-scale is significantly slower than that on macro scale.

The twin-shaft kneader is generally well-suited for devolatilization purposes due to fast surface renewal of high viscous fluids by kneading. It has to be taken into account if the component to be removed is dissolved or dispersed. Deodorization of remaining monomers after polymerization, resp. elimination of dispersed by-products, e.g. water, in case of polycondensation can be described by two film theory.

The presented methods offer the opportunity for investigation of the influence of the structural shape on the twin-shaft kneader's performance.

[1] E. L. Paul, "*Handbook of Industrial Mixing*", J. Wiley & Sons, **1980**.
[2] N.n., "NPE Preview". *Plastics Additives and Compounding*, **2009**, *11*, 28–31.
[3] P. A. Fleury, "Bulkpolimerization of Methyl Methacrylat in a Kneader Reactor", Annual Technical Conference (ANTEC) Charlotte, NC, USA May 7-11, **2006**.
[4] B. T. Safrit, A. E. Diener, "Kneadertechnology for the Direct Devolatilization of Temperature Sensitive Elastomers", Annual Technical Conference (ANTEC) Milwaukee, WI, USA May 4–6, **2008**.
[5] A. Zabaleta, I. González, J. I. Eguiazábal, J. Nazábal, "Rubber toughening of Poly(ether imide) by Modification with Poly(butylene terephthalate)". *European Polymer Journal*, **2009**, *45*, 466–473.
[6] Shyh-shin. Hwang, Peming P. Hsu, Jui-ming. Yeh, Jui-pin. Yang, Kung-chin. Chang, Ying-zhong. Lai, "Effect of Clay and Compatibilizer on the Mechanical/Thermal Properties of Microcellular Injection Molded Low Density Polyethylene Nanocomposites". *International Communications in Heat and Mass Transfer*, **2009**, *36*, 471–479.
[7] Worawan Pechurai, Charoen Nakason, Kannika Sahakaro, "Thermoplastic Natural Rubber Based on Oil Extended NR and HDPE Blends: Blend Compatibilizer. *Phase Inversion Composition and Mechanical properties" Polymer Testing*, **2008**, *27*, 621–631.
[8] Berenika Hausnerova, Tomas Sedlacek, Pavlina Vltavska, "Pressure-Affected Flow Properties of Powder Injection Moulding Compounds". *Powder Technology*, **2009**, *194*, 192–196.
[9] Yusuke Shibata, Makiko Fujii, Yuka Sugamura, Ryusuke Yoshikawa, Shinji Fujimoto, Sayaka Nakanishi, Yuya Motosugi, Naoya Koizumi, Masaki Yamada, Kiyohisa Ouchi, Yoshiteru Watanabe, "The Preparation of a Solid Dispersion Powder of Indomethacin with Crosspovidone Using a Twin-Screw Extruder or Kneader". *International Journal of Pharmaceutics*, **2009**, *365*, 53–60.
[10] Ming-Shyan Huang, Hung-Chuan Hsu, "Effect of Backbone Polymer on Properties of 316L Stainless Steel MIM Compact". *Journal of Materials Processing Technology*, **2009**, *209*, 5527–5535.
[11] E. J. Troelstra, L. L. V. Dierendonck, D. L. P. B. M. Janssen, S. Maeder, A. Renken, "Radical Addition Polymerisation of Acrylates in a Buss-kneader". *Chemical Engineering Science*, **1996**, *51*, 2479–2488.
[12] F. Apruzzese, J. Pato, S. T. Balke, L. L. Diosady, "Inline Measurement of Residence Time Distribution in a Co-Rotating Twin-Screw Extruder". *Food Research International* **2003**, *36*, 461–467.

[13] Unlu Emine, James F. Faller, ''RTD in Twin-Screw Food Extrusion''. *Journal of Food Engineering* **2002**, *53*, 115–131.
[14] M. K. RazaviAghjeh, H. Nazokdast, H. Assempour, ''Determination of the Residence Time Distribution in Twin Screw Extruders via Free Radical Modification of PE''. *Intern. Polym. Process.* **2004**, *19*, 335–341.
[15] J. P. Puanx, G. Bozga, A. Ainser, ''Residence Time Distribution in a Corotating Twin Screw Extruder – a Review''. *Chemical Engineering Science*, **2000**, *55*, 1641–1651.
[16] A. Poulesquen, B. Vergnes, ''A Study of Residence Time Distribution in Co-Rotating Twin-Screw Extruders''. *Polymer Engineering and Science*, **2003**, *43*, 1849–1862.
[17] Xian-Ming Zhang, Zhong-Bin Xu, Lian-Fang Feng, Xiao-Bo Song, Guo-Hua Hu, '' Assessing Local Residence Time Distributions in Screw Extruders Through a New In-Line Measurement Instrument''. *Polymer Engineering and Science*, **2006**, *46*, 510–519.
[18] K. Shon, D. Chang, und J. L. White, ''A Comparative Study of Residence Time Distributions in a Kneader, Continuous Mixer, and Modular Intermeshing Co-Rotating and Counter-Rotating Twin Screw Extruders'' *Int. Polym. Process*, **1999**, *14*, 44–50.
[19] M. Y. Lyu, J. L. White, ''Residence Time Distributions and Basic Studies of Flow and Melting in a Modular Buss Kneader'' *Polym. Eng. Sci.* **1998**, *38*, 1366–1377.
[20] P. Vrabel, R. G. J. M. van der Lans, K. Ch. A. M. Luyben, L. Boon, A. W. Nienow, ''Mixing in Large-Scale Vessels Stirred with Multiple Radial or Radial and Axial Up-Pumping Impellers: Modeling and Measurments''. *Chemical Engineering Science*, **2000**, *55*, 5881–5896.
[21] E. S. Szalai, P. Arratia, K. Johnson, F. J. Muzzio, ''Mixing Analysis in a Tank Stirred with Ekato Intermig Impellers''. *Chemical Engineering Science*, **2004**, *59*, 3793–3805.
[22] T. K. Kang, M. K. Singh, T. H. Kwon, P. D. Anderson, ''Chaotic Mixing Using Periodic and Aperiodic Sequences of Mixing in a Micromixer''. *Microfluidics and Nanofluidics*, **2008**, *4*, 589–599.
[23] L. Yerramilli, M. V. Karwe, ''Velocity Distributions and Mixing in the Translational Region of a Kneading Section in a Co-rotating Twin-screw Extruder''. *Food and Bioproducts Processing*, **2004**, *82*, 5–12.
[24] E. C. Barnes, D. I. Wilson, M. L. Johns, ''Velocity Profiling Inside a Ram Extruder using Magnetic Resonance (MR) Techniques''. *Chemical Engineering Science*, **2006**, *61*, 1357–1367.
[25] Neil. P. Stuber, Matthew Tirrell, ''Continuous Polymerization Studies In A Twin-Screw Extruder''. *Polymer Process Engineering*, **1985**, *3*, 71–83.
[26] H. E. H. Meijer, P. H. M. Elemans, ''The Modeling of Continuous Mixers. Part I: The Corotating Twin-Screw Extruder'' *Polym. Eng. Sci.*, **1988**, *28*, 275–290.
[27] P. H. M. Elemans, H. E. H. Meijer, ''On the Modeling of Continuous Mixers. Part II: The Cokneader''. *Polym. Eng. Sci.*, **1990**, *30*, 893–904.
[28] M. Mehranpour, H. Nazokdast, B. Dabir, ''Prediction of Residence Time Distribution for Different Screw Configurations of a Ko-Kneader by using a Cluster Model''. *Intern. Polym. Process.*, **2004**, *14*, 13–15.
[29] P. G. M. Kruijt, O. S. Galaktionov, G. W. M. Peters, H. E. H. Meijer, The Mapping Method for Mixing Optimization. Part II: Transport in a Corotating Twin Screw Extruder. *Int. Polym. Proc.* **2001**, *16*, 161–171.
[30] Vincent Stobiac, Mourad Heniche, Christophe Devals, François Bertrand, Philippe Tanguy, ''A Mapping Method Based on Gaussian Quadrature: Application to Viscous Mixing''. *Chemical Engineering Research and Design*, **2008**, *86*, 1410–1422.
[31] J. Biesenberger, S. T. Lee, ''A Fundamental Study of Polymer Melt Devolatilization. Part I: Some Experiments on Foam-Enhanced Devolatilization''. *Polymer Engineering and Science*, **1986**, *14*, 982–988.
[32] R. W. Foster, J. T. Lindt, ''Twin Screw Extrusion Devolatilization: From Foam to Bubble Free Mass Transfer.'' *Polymer Engineering and Science*, **1990**, *11*, 621–633.
[33] I. Gestring, D. Mewes, ''Degassing of Molten Polymers''. *Chemical Engineering Science*, **2002**, *57*, 3415–3426.
[34] R. M. Secor, ''A Mass Transfer Model for a Twin Screw Extruder''. *Polymer Engineering Science*, **1986**, *26*, 647–652.
[35] N. H. Wang, T. Sakai, N. Hashimoto, ''Modeling of Polymer Devolatilization in a Multi-Vent Screw Extruder''. *International Polymer Processing*, **1995**, *4*, 296–304.
[36] C.-T. Yang, T. G. Smith, D. I. Bigio, C. Anolick, ''Polymer Trace Devolatilization: I. Foaming Experiments and Model Development''. *AIChE Journal*, **1997**, *7*, 1861–1873.
[37] C.-T. Yang, T. G. Smith, D. I. Bigio, C. Anolick, ''Polymer Trace Devolatilization: II. Case Study and Experimental Verification'' *AIChE Journal*, **1997**, *7*, 1874–1883.
[38] O. Levenspiel, ''*Chemical Reaction Engineering*'', 3rd Edition, J. Wiley & Sons, **1998**, *13*, 293 ff
[39] W. G. Whitman, *Chem. Metall. Eng.* **1923**, *29*, 147.
[40] W. K. Lewis, W. G. Whitman, *Chem Metall. Eng.* **1924**, *16*, 1215
[41] N.N., Datablatt 2-Nitrophenol, Landesamt für Umwelt, Messung und Naturschutz Badenwürtemberg

